ELSEVIER

Journal of Nuclear Materials 294 (2001) 148–153

journal of nuclear materials

www.elsevier.nl/locate/jnucmat

The oxidation kinetics and the structure of the oxide film on Zircaloy before and after the kinetic transition

T. Arima *, T. Masuzumi, H. Furuya, K. Idemitsu, Y. Inagaki

Institute of Environmental Systems, Kyushu University, Fukuoka 812-8581, Japan

Abstract

Oxidation kinetics of Zircaloy-4 have been measured using a micro-balance technique in $CO–CO_2$ gas mixtures between 450°C and 600°C. Oxidation kinetics of Zircaloy-4 obeyed a cubic rate law with time at 450–600°C up to 24 h. At 600°C, the kinetic transition occurred after about 36 h. After the transition, oxidation kinetics obeyed a linear rate law. X-ray diffraction patterns for the samples oxidized at 600°C showed that the volume fraction of tetragonal phase of zirconia decreased with time until the kinetic transition occurred and was almost constant after that. In addition, stresses in the oxide films were found to be larger for the pre-transition samples than for the post-transition ones.

PACS: 28. 41. T; 81. 65. M

1. Introduction

The so-called 'kinetic' transition of Zircaloy oxidation, that is, when oxidation becomes accelerated, needs to be better understood for nuclear reactor safety. Recently, some light water reactor (LWR) fuels have been irradiated to a burn-up of over 50 GWd/t. Furthermore, mixed-oxide fuels (MOX) have begun to be loaded into LWRs. Under such conditions, the oxidation rate of Zircaloy claddings is expected to be accelerated on the fuel-side as well as on the coolant-side.

The oxidation behavior of Zircaloy-2 in terms of oxygen partial pressure was reported in our previous study [1]. In that article, we showed that oxidation was not dependent on oxygen partial pressure in the pre-transition period and concluded that diffusion of oxygen vacancies controlled the oxidation rate. On the other hand, in the post-transition period, the oxidation rate was been found to be dependent on oxygen partial pressure in some reports [2,3]. The authors argued that the oxidation behavior was caused by interstitial oxygen and by imperfect oxide films, i.e., cracks and pores. In recent studies by Godlewski et al. [4,5], the kinetic transition was discussed in terms of the lattice structure of oxide films. They pointed out that the kinetic transition was accompanied by the tetragonal-to-monoclinic phase transition of the oxide film.

In this study, the dependence of the oxidation rate of Zircaloy-4 on both the oxygen partial pressure (10^{-30}–10^{-2} atm) and temperature (450–600°C) has been measured by a micro-balance technique. In addition, X-ray diffractometry (XRD) and scanning electron microscopy (SEM) were performed for the oxide films. The relationship between the oxidation kinetics and the structure of oxide film is discussed on the basis of data obtained by these measurements.

2. Experimental

The specimens of Zircaloy-4 used in this experiment were cut from α-forged rod into disks of 10 mm diameter and 0.5 mm thickness. The specimen surfaces were polished on abrasive papers and then subsequently finished by alumina buffing.

The oxidation experiments were carried out using a micro-balance apparatus (Cahn-2000) between 450°C

* Corresponding author. Tel.: +81-92 642 3779; fax: +81-92 642 3800.

E-mail address: arima@nucl.kyushu-u.ac.jp (T. Arima).

0022-3115/01/$ - see front matter
PII: S0022-3115(01)00453-6

and 600°C. The desired oxygen partial pressure in the reaction system was obtained by changing the composition of the flowing gas components, i.e., 0–5% CO/CO_2. These gases were supplied at 50 ml/min under atmospheric pressure, and the oxygen partial pressures were monitored by a calcia stabilized zirconia sensor. The experimental method for thermo-gravimetry was described in our previous report [1].

In order to investigate the relationship between the oxidation kinetics and the structure of the oxide film, X-ray diffraction measurements were performed. X-ray patterns from oxide films were acquired using an XD-D1 Shimadzu diffractometer. The diffractometer was used with Cu-Kα radiation and at conditions of 30 keV and 30 mA. All X-ray diffraction measurements were performed at room temperature. Thus, the volume fraction of tetragonal-to-monoclinic zirconia as well as the stress in the oxide film was analyzed as a function of time. The quantities of tetragonal and monoclinic zirconia in the oxide film were evaluated using the areas of the $(1\,1\,1)_t$, $(\bar{1}\,1\,1)_m$ and $(1\,1\,1)_m$ peaks. This semi-analytic method was proposed by Garvie and Nicholson [6].

The stress generated in the oxide films can be evaluated from the change of plane spacing d as a function of ψ, which is angle between sample surface and diffracted plane. Here, changing ψ in the range 0–15°, the plane spacing d for the monoclinic $(\bar{4}\,0\,1)$ peak was measured to derive the stress [7]. In practice, the diffraction angle $2\theta_\psi$ corresponding to the monoclinic $(\bar{4}\,0\,1)$ peak was used to derive the stress.

For the SEM examinations, the cross-sections of oxidized samples embedded in a acrylic resin were observed. The surfaces of the observed sections were mechanically polished as described above, then chemically polished using a swabbing-technique with a solution of 10 vol.% HF, 45 vol.% HNO_3, and 45 vol.% H_2O. Finally, these surfaces were coated with gold.

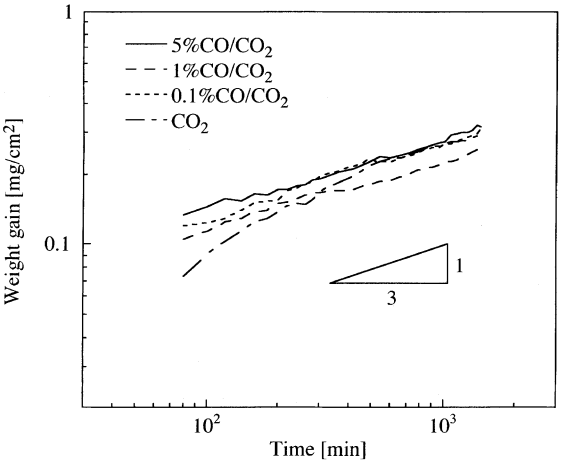

Fig. 1. Weight gain curves of Zircaloy-4 disk at 500°C for 24 h.

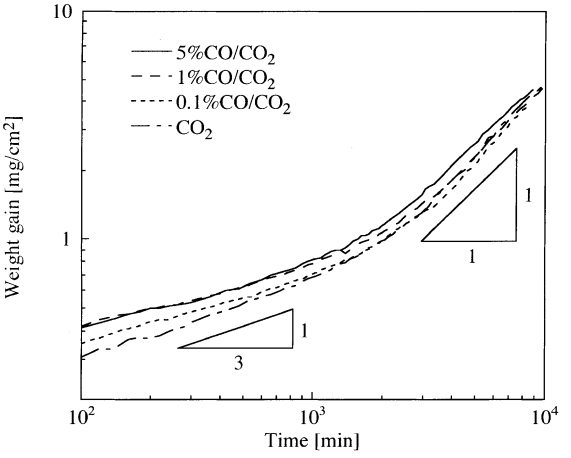

Fig. 2. Weight gain curves of Zircaloy-4 disk at 600°C for 7 days.

3. Results and discussion

3.1. Oxidation kinetics

The weight change of specimens were measured as a function of time with the micro-balance. The weight gains per unit area in atmospheres of 0–5% CO/CO_2 at 500°C for 24 h (Fig. 1) show that the weight gains for all the gas atmospheres increase with time while keeping a constant slope. This means there was no occurrence of the kinetic transition. For conditions of 450°C and 550°C up to 24 h, both weight gains also show similar tendency to that of 500°C. Fig. 2 shows the weight gain curves at 600°C for 7 days. The kinetic transition points are found at about 36 h on the weight gain curves where the slope changes from 3 to 1. At 600°C, the oxidation kinetics of Ziraloy-4 follows a cubic rate law before the transition and a linear rate law after the transition.

In general, for oxidation kinetics, the cubic rate law and the linear rate law are given by

$$W^3 = k_C t, \tag{1}$$

$$W = k_L t, \tag{2}$$

where k_C and k_L are the cubic and linear rate constants, respectively. For the oxidation condition of 450–600°C and 24 h, k_C increase with oxidation temperature though its oxygen partial pressure dependence cannot be found. The activation energies were calculated to be 150–210 kJ/mol using the Arrhenius relation between the rate constant and temperature. Such results were also seen in our previous study of Zircaloy-2 [1]. On the other hand, for oxidation at 600°C and over 36 h, the rate constant k_L does not show a dependence on oxygen partial

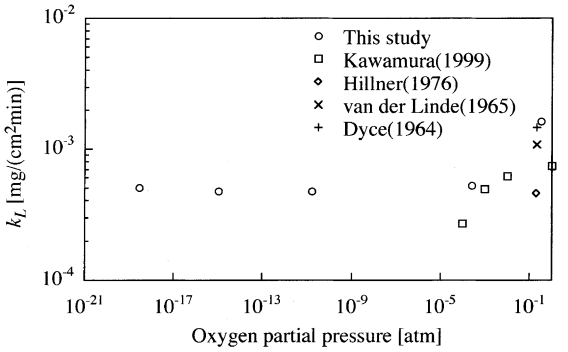

Fig. 3. The effect of oxygen partial pressure on the linear rate constant of oxidation of Zircaloy-4 at 600°C. The rate constants of the other oxidation experiments are derived from each figure in [3,8].

pressure either. In other experiments, dependence on oxygen partial pressure at high oxygen partial pressures is sometimes seen in the linear rate constant in a high oxygen partial pressure regime [2,3]. So we performed oxidation experiments at the high oxygen partial pressure of Ar–20%O_2. Our results, as well as those obtained by others [3,8] are shown in Fig. 3. These results may indicate that at the low oxygen partial pressure achieved in CO–CO_2 gas mixtures, oxidation kinetics are controlled by the diffusion of oxygen vacancies whereas at high oxygen partial pressures, interstitial diffusion of oxygen may be the predominant process of oxidation.

3.2. Tetragonal-to-monoclinic phase ratio

Figs. 4((a)–(c)) show the X-ray diffraction patterns of samples heated in CO_2 at 450°C for 24 h and 600°C for 7 days. All diffraction patterns shown in these figures were measured by using the $2\theta - \theta$ method. Most peaks from the oxidized samples originated from m (monoclinic)-ZrO_2 and α (hexagonal)-Zr. The small peaks near $2\theta = 30°$ indicate the existence of t (tetragonal)-ZrO_2. No α-Zr peaks can be seen in Fig. 4(c) which shows samples that have undergone the kinetic transition.

A peak intensity $I(hkl)_i$ can be defined as the intensity of the (*hkl*) diffraction line of phase *i*. In this analysis, peak intensities were calculated by fitting the diffraction line to a Gaussian function. The peak intensity ratio of the tetragonal phase X_t is expressed by

$$X_t = \frac{I(1\,1\,1)_t}{I(\bar{1}\,1\,1)_m + I(1\,1\,1)_m + I(1\,1\,1)_t}, \tag{3}$$

as given by Garvie and Nicholson [6]. The X_t thus obtained is equal to the volume fraction of the tetragonal phase within a few %. The volume fraction of the tetragonal phase V_t is described more precisely by the following expression:

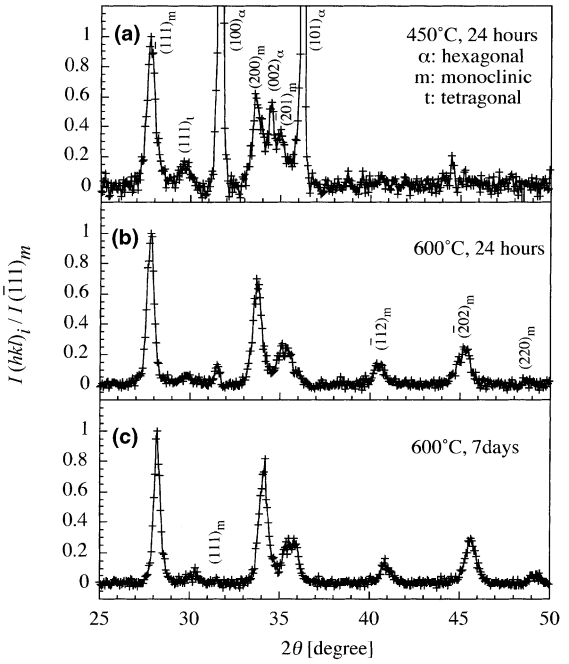

Fig. 4. X-ray diffraction patterns of specimens oxidized in CO_2 (a) at 450°C, 24 h; (b) at 600°C, 24 h; (c) at 600°C, 7 days. Ordinate is the X-ray intensity normalized by the $(\bar{1}\,1\,1)_m$ peak intensity. Background intensities were subtracted.

$$V_t = \frac{X_t}{C(1 - X_t) + X_t}, \tag{4}$$

where $C = 1.381$ for Cu-Kα [9]. The value of C includes several factors concerning the intensity of diffracted X-rays, e.g., structure factor, multiplicity and Lorentz polarization factor.

Fig. 5 shows the volume fraction of the tetragonal phase V_t as a function of time. All samples in this figure were oxidized in a 5% CO/CO_2 atmosphere. For both

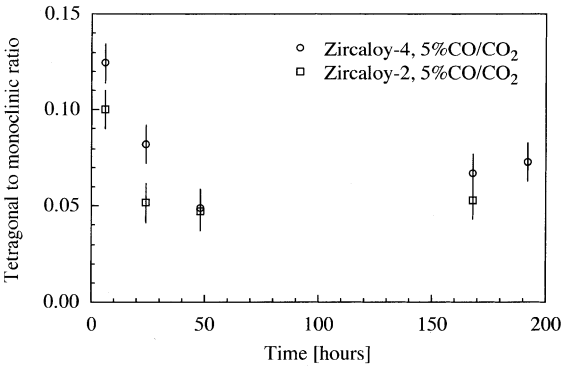

Fig. 5. Volume ratio of tetragonal-to-monoclinic zirconia as a function of oxidation time.

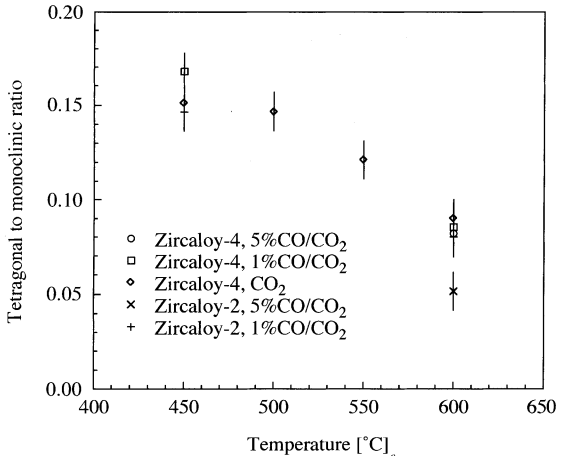

Fig. 6. Volume ratio of tetragonal-to-monoclinic zirconia as a function of oxidation temperature for 24 h heat treatments.

Zircaloy-4 and -2 samples, V_t monotonically decreased with increasing oxidation time until the kinetic transition was reached, and remained constant within about 6% after that point. In Fig. 6, the V_t of samples oxidized for 24 h is plotted as a function of temperature. The figure shows that the lower the temperature, the larger the volume fraction of tetragonal phase.

Fig. 7 shows the relationship between V_t and thickness of the oxide film. It shows that large V_t can only be found in the pre-transition period. The main reason for these results is usually due to the high Pilling–Bedworth ratio of 1.56 for zirconium. According to the pressure–temperature phase diagram of zirconia [10], the tetragonal phase is stabilized by the higher stress. However,

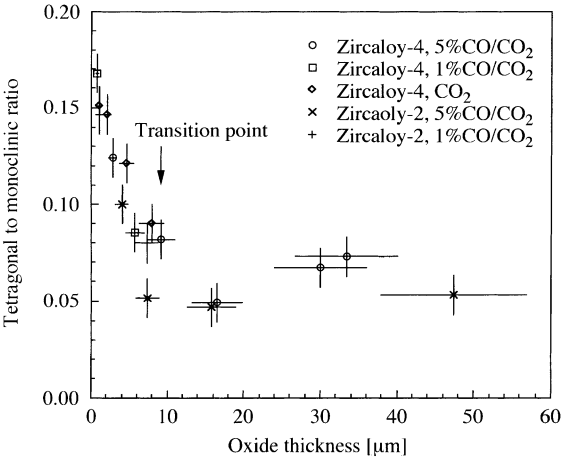

Fig. 7. Volume ratio of tetragonal-to-monoclinic zirconia as a function of oxide thickness. The oxide thickness was calculated using the conversion formula 1.5 mg/dm^2 = 100 nm. Data shown in Figs. 5 and 6 are included in this figure.

the X-ray penetration lengths must be considered to help understand these results. The penetration length (95%) is estimated to be ~6 μm for zirconia. Since samples oxidized at 600°C, or less, for less than 24 h showed the diffraction peak from underlying zirconium, and the oxide thickness was comparable with the penetration length, X-ray information for the pre-transition samples resulted from whole area of oxide film. On the other hand, for the post-transition samples, only the thick surface oxide layers were seen by X-rays because its oxide thickness was much thicker than the X-ray penetration length. These samples had V_t values of about 6%, neglecting the metal–oxide interface where high stress occurred. Therefore, for the post-transition samples, the tetragonal phase may have been stabilized, not due to high P–B ratio, but for another reason, such as an oxide grain size effect [11].

The abscissa of Fig. 7 shows the thickness of oxide film, which was calculated using a conversion formula between weight gain and thickness, 1.5 mg/dm^2 = 100 nm. The oxide thickness error was conservatively estimated to be ±20%. The error of V_t was estimated to be ±0.01.

3.3. Stress measurement

The stresses in the oxide film and the zirconia phase were evaluated by X-ray diffraction measurements. To simplify the following discussion, the calculation of the stress has been carried out under the assumptions of isotropy and homogeneity of the oxide. In addition, the stress component normal to the surface of the specimen was considered to be zero. Thus, on the basis of the theory of the X-ray stress measurement, the stress generated in the oxide film can be written by

$$\sigma_x = -\frac{E\cot\theta_0}{2(1+v)}\frac{\partial 2\theta_\psi}{\partial \sin^2\psi}, \tag{5}$$

where E is Young's modulus, v is Poisson's ratio, and θ_0 is the diffraction angle under the non-stress condition.

In Fig. 8, the diffraction angles $2\theta_\psi$ are plotted as a function of $\sin^2\psi$ for the samples oxidized under 1% and 5% CO/CO_2 atmospheres. The slopes determined for all oxidized samples are positive. This means that compressive stress exists in the oxide film. In addition, the slopes for the pre-transition samples are larger than those for the post-transition ones, which means that higher compressive stress in the oxide film existed in the pre-transition sample. However, for the underlying zirconium, a negative slope value was obtained. For the samples oxidized under the different experimental conditions, the values of slopes determined from the $2\theta_\psi - \sin^2\psi$ plot are shown in Fig. 9 as a function of the oxidation time. This figure also shows larger slopes for pre-transition samples. The errors indicated in this figure resulted mainly from statistical analysis, and these

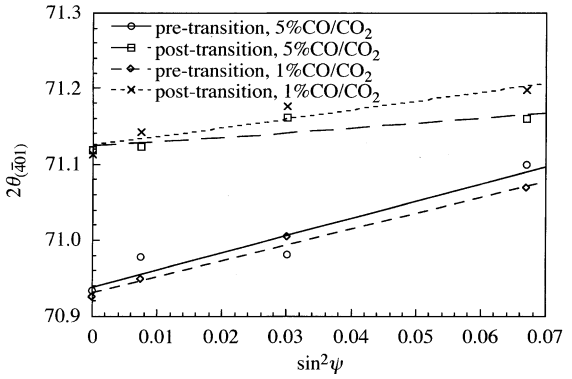

Fig. 8. Scattering angle corresponding to monoclinic zirconia $(\bar{4}01)$ peak as a function of ψ. The angle ψ is the angle between the sample surface and the diffraction plane.

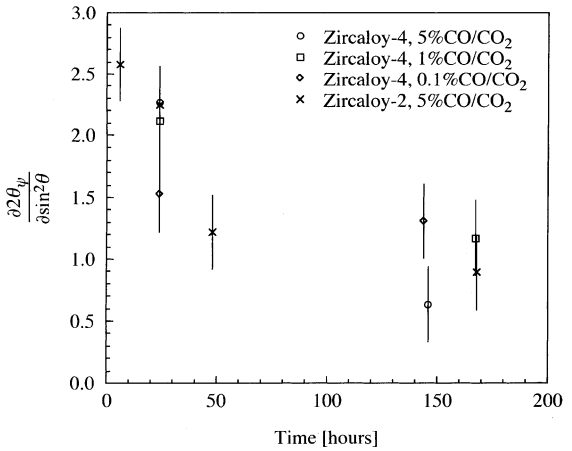

Fig. 9. Slopes calculated from the $2\theta_\psi$–$\sin^2\psi$ plot as a function of the oxidation time. They are proportional to the magnitude of the stress in the oxide film.

values were conservatively estimated to be ± 0.3. Using $E = 200$ GPa and $v = 0.3$ [12,13], the compressive stresses in the oxide films were about 4 and 2 GPa for pre-transition and post-transition samples, respectively. The maximum value of compressive stress about 4 GPa is higher than those obtained by others experiments [5,7,14]. They explain that lower compressive stress does not include the information from the metal/oxide interface, and that zirconia with high concentration of tetragonal phase is stabilized by dopant atoms [4]. According to the P–T phase diagram of zirconia, the transition pressure of monoclinic-to-tetragonal or to orthorhombic phase decreases with increasing temperature and changes form 3.5 GPa (room temperature) to 2 GPa (600°C). The maximum stress value obtained in our experiment was higher than values shown in the P–T phase diagram.

3.4. SEM examination

Figs. 10 ((a) and (b)) show SEM photographs of oxide films formed on specimens heated in 5% CO/CO_2 at 600°C for 24 h and 8 days. The specimen oxidized for 8 days showed the kinetic transition point on its weight gain curve. For other atmospheric conditions, similar results were obtained. In these figures, two types of cracks are found in oxide films. Lateral cracks, parallel to the specimen surface, are observed in all oxide films. For the post-transition period films, vertical cracks, normal to the surface of specimen, are found. And, as shown in Fig. 10(b), the vertical cracks are often observed at thicker parts of oxide films.

The shape of the interface between the oxide film and the underlying metal is wavy rather than flat, which results from the varying oxidation rate with position. This tendency was found for all oxidized samples. Zircaloy-2 samples also showed the same tendency in our previous study [1].

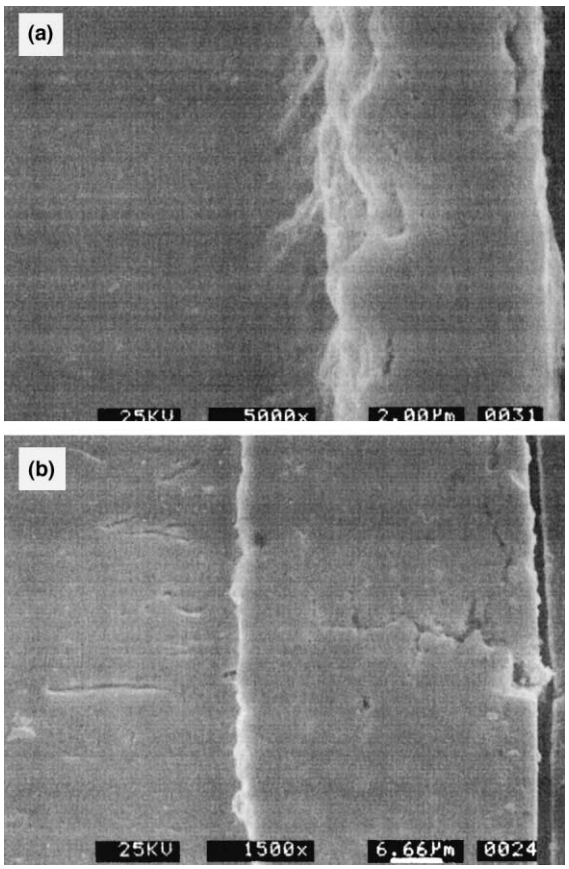

Fig. 10. SEM photographs of oxide film formed on Zircaloy-4 in 5% CO/CO_2 at 600°C for (a) 24 h, (b) 8 days. The oxide films are on the right of the underlying metal in each figure.

Vertical cracks are considered to promote oxidation since these cracks are relatively large diffusion paths for the oxidizing gas and are directly opened to the atmosphere. On the other hand, almost all lateral cracks are smaller than the vertical ones and are closed in the oxide film. Therefore, the wavy shape of metal–oxide interface may be due to closed lateral cracks preventing the oxidation reaction [15,16]. But, if the lateral cracks connect each other and reach the surface, they may play the same role as vertical ones.

4. Summary

The oxidation kinetics of Zircaloy-4 have been studied between 450°C and 600°C under the atmospheres of 0–5% CO/CO_2 gas mixtures. For the oxidized sample, X-ray diffraction was used to investigate the relationship between the kinetic transition and the lattice structure of oxide films.

The oxidation of Zircaloy-4 obeyed a cubic rate law in the pre-transition period and a linear rate law in the post-transition period. Under low oxygen partial pressures such as those achieved in $CO–CO_2$ gas mixtures, both kinetic rate constants were insensitive to oxygen partial pressure whereas under high oxygen partial pressures, the linear rate constant seemed to depend on oxygen partial pressure.

From the analysis of ratios of tetragonal-to-monoclinic phases in the oxide film, the pre-transition samples had higher tetragonal phase ratios (over 10%). For samples oxidized up to 24 h, the tetragonal phase ratios decreased with increasing temperature. The post-transition samples had a tetragonal phase ratio of about 6%, which indicated that the tetragonal phase was stabilized, but the cause did not seem to be high *P–B* ratio.

Stresses generated in oxide films were estimated from the $2\theta_\psi - \sin^2\psi$ plots. The stresses for all oxidized samples were compressive, and these values were about 4 and 2 GPa for the pre- and post-transition samples, respectively. For the pre-transition samples, high values of stresses as well as high tetragonal phase ratios resulted from the high P–B ratio of 1.56 for zirconium.

SEM photographs of oxidized samples indicate that lateral cracks, found for all oxide films, may inhibit the oxidation reaction at the metal/oxide interface and decrease the oxygen diffusion paths, whereas vertical cracks found for post-transition samples promotes oxidation.

Acknowledgements

The authors gratefully acknowledge the continuous support of the technical staff, M. Momoda and M. Kutsuwada. We also wish to thank M. Watanabe of the Center of Advanced Instrumental Analysis, Kyushu University, for her help with the X-ray diffraction measurements.

References

[1] T. Arima, K. Moriyama, N. Gaja, H. Furuya, K. Idemitsu, Y. Inagaki, J. Nucl. Mater. 257 (1998) 67.
[2] J. Nakamura, M. Hashimoto, T. Otomo, S. Kawasaki, J. Nucl. Mater. 200 (1993) 256.
[3] K. Kawamura, A. Kaimai, Y. Nigara, T. Kawada, J. Mizusaki, J. Electrochem. Soc. 146 (1999) 1608.
[4] J. Godlewski, J.P. Gros, M. Lambertin, J.F. Wadier, H. Weidinger, Zirconium in the Nuclear Industry, in: C.M. Euken, A.M. Garde (Eds.), ASTM-STP 1132, ASTM, Philadelphia, 1991, pp. 416–433.
[5] J. Godlewski, Zirconium in the Nuclear Industry, in: A.M. Garde, E.R. Bradley (Eds.), ASTM-STP 1245, ASTM, Philadelphia, PA, 1994, pp. 663.
[6] R.C. Garvie, P.S. Nicholson, J. Am. Ceram. Soc. 55 (1972) 303.
[7] C.H. Valot, D. Ciosmak, M.T. Mesnier, E. Sciora, M. Lallemant, J.J. Heizmann, A. Vadon, C. Laruelle, J. Phys. IV, Colloq. 6 (C4) (1996) 279.
[8] E. Hillner, Zirconium in the Nuclear Industry, in: A.L. Lowe, G.W. Parry (Eds.), ASTM-STP 633, ASTM, Philadelphia, PA, 1977, pp. 211.
[9] R. Fillit, P. Homerin, J. Schafer, H. Bruyas, F. Thevenot, J. Mater. Sci. 22 (1987) 3566.
[10] H. Arashi, M. Ishigame, Phys. Stat. Sol. 71 (1982) 313.
[11] P. Barberis, J. Nucl. Mater. 226 (1995) 34.
[12] S.K. Chan, Y. Fang, M. Grimsditch, Z. Li, M.V. Nevitt, W.M. Robertson, E.S. Zouboulis, J. Am. Ceram. Soc. 74 (1991) 1742.
[13] R.E. Cohen, M.J. Mehl, L.L. Boyer, Phys. B 150 (1988) 1.
[14] C. Roy, B. Burgess, Oxid. Met. 2 (1970) 235.
[15] J.P. Pemsler, J. Electrochem. Soc. 112 (1965) 477.
[16] B. Hutchinson, B. Lehtinen, J. Nucl. Mater. 217 (1994) 243.